Photonic design principles for ultrahigh-efficiency photovoltaics

Albert Polman and Harry A. Atwater

For decades, solar-cell efficiencies have remained below the thermodynamic limits. However, new approaches to light management that systematically minimize thermodynamic losses will enable ultrahigh efficiencies previously considered impossible.

Ever since serious scientific thinking went into improving the efficiency of photovoltaic energy conversion more than 50 years ago, thermodynamics has been used to assess the limits to performance, guiding advances in materials science and photovoltaic technology. On the basis of this approach, photovoltaic technology has advanced considerably, resulting in single-junction solar cells with a record efficiency of 28.3% (ref. 1) and multi-junction cells with an efficiency (under concentrated illumination) of 43.5% (ref. 2). Worldwide photovoltaic manufacturing capacity is expected to surpass 40 gigawatts per year in 2012, and is steadily growing[3]. The cell efficiencies for most of this manufactured output, however, remain in the 10–18% range. As impressive as these advances are, these record efficiencies and the manufactured cell efficiencies fall far short of the thermodynamic limits to photovoltaic energy conversion.

Why such a large gap? We suggest that there is no fundamental reason, and that by systematically addressing the thermodynamic efficiency losses in current photovoltaics, a next phase of photovoltaic science and engineering —ultrahigh-efficiency photovoltaics — is at hand. This development takes advantage of recent advances in the control of light at the nanometre and micrometre length scales, coupled with emerging materials fabrication approaches, and will allow the development of solar cells with efficiencies in the 50–70% range.

Our approach addresses opportunities for efficiency increases within the guiding assumptions outlined by Shockley and Queisser in 1961[4], namely the creation of one thermalized electron–hole pair per absorbed photon above the semiconductor bandgap of the photovoltaic absorber. It does not involve use of what has been termed third-generation photovoltaics, which extends in scope beyond the Shockley–Queisser limit, including solar cells exploiting multiple-exciton generation, hot-carrier collection, upconversion, downconversion and intermediate-band photovoltaics[5,6]. These too are exciting scientific developments that have potential to eventually result in high-efficiency photovoltaics, although considerable scientific effort is still required before a clear prospect for high-efficiency photovoltaics emerges from these concepts.

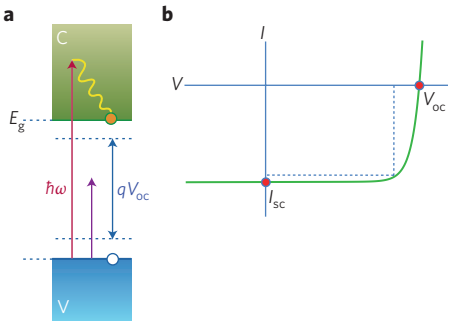

Figure 1 | Solar-cell characteristics. **a**, Energy diagram of a single-junction solar cell. Light at an energy $\hbar\omega$ (red arrow) creates an excitation from the valence (V) to the conduction (C) band of a semiconductor. After thermalization in the conduction band an electron–hole pair is formed across the bandgap with energy E_g. Light with an energy below the bandgap (purple arrow) is not absorbed. **b**, Typical current–voltage (I–V) characteristics of a solar cell. The short-circuit current I_{sc} is a direct measure of the conversion efficiency from incident photons to electrical current. The open-circuit voltage V_{oc} is determined by the factors described in the main text; it is significantly lower than E_g due to entropic reasons. The maximum-power operating point of the solar cell is indicated by the dashed lines.

Two basic elements arise in a thermodynamic analysis of high-efficiency photovoltaics within the Shockley–Queisser model: (1) reducing the deficit between the bandgap energy and the electron–hole quasi-Fermi-level splitting, and (2) minimization of carrier thermalization losses and absorption-loss of sub-bandgap light (Fig. 1). The separation of the electron and hole quasi-Fermi levels qV_{oc} defines the maximum achievable open-circuit voltage V_{oc} of the cell. Maximizing V_{oc} is key towards achieving high conversion efficiencies. In the radiative recombination limit, assuming full collection of all generated carriers, and assuming a semiconductor structure in the ray optics limit, V_{oc} is less than the bandgap energy E_g according to:

$$qV_{oc} = E_g\left(1 - \frac{T}{T_{sun}}\right) - kT\left[\ln\left(\frac{\Omega_{emit}}{\Omega_{sun}}\right) + \ln\left(\frac{4n^2}{I}\right) - \ln(QE)\right] \quad (1)$$

The first term on the right represents the conversion of the energy of photons with $E_g=\hbar\omega$ (where ω is frequency) to electrostatic energy and includes fundamental thermodynamic losses based on Carnot's theorem, where T is the solar-cell temperature and T_{sun} is the temperature of the Sun. This reduces V_{oc} by 5% compared with E_g at room temperature. Further accounting for loss of energy through photon spontaneous emission rather than blackbody radiation modifies this first term, giving rise to loss of another 7% (ref. 7). This

photon-loss component could in principle be overcome by design of non-reciprocal photonic structures. We also note that equation (1) addresses the open-circuit voltage, whereas a solar cell must have an operating point voltage that maximizes power transfer to an external circuit; solar-cell operation at the operating point voltage incurs a loss of ~100 meV to the open-circuit voltage.

The term in square brackets accounts for three entropy-related terms. The first term reflects the entropy increase on photon absorption and re-radiation through spontaneous emission in a semiconductor; whereas an incoming photon from the direct solar spectrum is incident within a solid angle of $\Omega_{sun} = 6 \times 10^{-5}$ steradians, outgoing photons radiated through spontaneous emission are emitted into a solid angle up to $\Omega_{emit} = 4\pi$ (refs 8–11). The increased entropy of light corresponds to a reduction in V_{oc} as large as 315 mV at room temperature. Thus, if photonic structures could be designed to limit the angle of radiative emission from the solar absorber to a solid angle approaching Ω_{sun}, a large fraction of this entropic energy loss could be avoided.

The second term, $\ln(4n^2/I)$, where n is the refractive index and I is the light concentration factor, describes the effect of incomplete light trapping inside the solar cell and is particularly relevant for light at an energy just above E_g that is poorly absorbed[12]. In a planar cell with no light trapping $I \equiv 1$, and this term reflects a loss in V_{oc} of 100 mV. Conventional solar cells also have a surface texture that leads to multiple internal reflection of light inside the semiconductor slab, enhancing the light intensity relative to that of a planar slab by a factor I. For cells in the classical ray optical limit, the maximum value of I that can be achieved is $4n^2$ so this entropy term vanishes[13]. Recent advances in the nanostructuring of solar-cell surfaces and back contacts have demonstrated light trapping beyond the $4n^2$ limit in a certain spectral range[14,15]. Light trapping also enhances the photocurrent of the cell.

The last term in the square brackets accounts for the loss in V_{oc} owing to non-radiative exciton recombination, which occurs because of crystallographic defects, impurities and other carrier traps in the bulk, at interfaces and at the surface. The quantum efficiency for radiative recombination is defined by $QE = R_{rad}/(R_{rad} + R_{nrad})$ where R_{rad} and R_{nrad} are the radiative and non-radiative recombination rates, respectively. For example, for the indirect-bandgap semiconductor silicon, QE generally is well below 10%, which translates into a reduction in V_{oc} of over 60 mV. Although a reduced QE is directly related to electronic materials properties, such as the density of carrier traps or surface recombination sites, it can be enhanced for a given materials geometry by enhancing R_{rad} through optical means: using wavelength-scale and subwavelength nanophotonic structures the local density of optical states can be artificially increased, which in turn leads to an increased R_{rad}. The enhanced QE then directly translates in an increased V_{oc}.

The three entropic loss terms described above result in a systematic reduction in V_{oc} below E_g. Indeed, V_{oc} is some 400–500 mV below E_g for nearly all practical solar-cell materials[1], indicating there is significant room for efficiency improvement if these loss factors could be minimized. Interestingly, each of these factors concern the control over the propagation of light inside the solar cell. Indeed, after 50 years of research and technical developments in the perfection of the electronic quality of photovoltaic materials, the key challenge now, and one that has great potential, is to better engineer the flow of light inside a solar cell.

In the 'conventional' Shockley–Queisser limit, with QE = 1 and full light absorption and trapping, the maximum achievable efficiency is 33% for a single-junction cell with a bandgap that is optimized for the solar spectrum (E_g = 1.4 eV, close to the bandgap for GaAs). As argued above, with further light-management strategies to redirect light back at the angle corresponding to the disk of the Sun, V_{oc} can be increased by several 100 mV so that an efficiency for a single-junction solar cell beyond 40% is achievable. Until now, such a high efficiency has only been achieved using triple-junction solar cells[1], here we outline that it can also be achieved using a

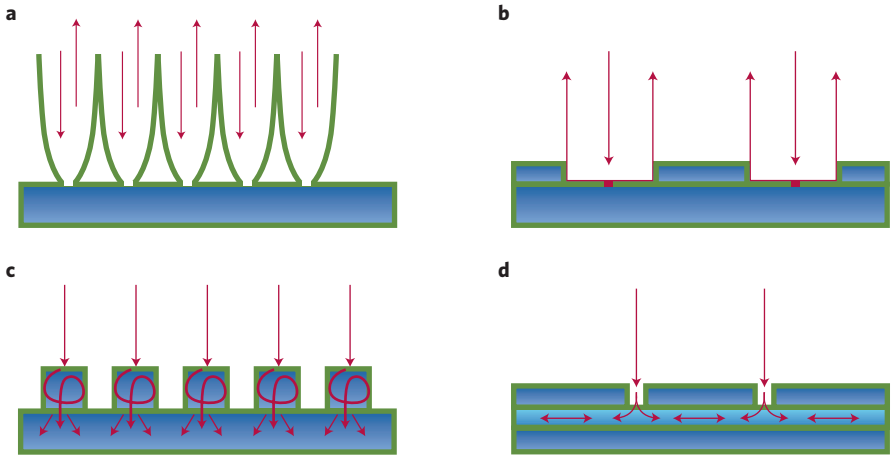

Figure 2 | Light-management architectures for reaching ultrahigh efficiency. **a**, Three-dimensional parabolic light reflectors direct spontaneous emission back to the disk of the Sun. **b**, Planar metamaterial light-director structures. **c**, Mie-scattering surface nanostructure for light trapping. **d**, Metal–dielectric–metal waveguide or semiconductor–dielectric–semiconductor slot waveguide with enhanced optical density of states to increase the spontaneous emission rate.

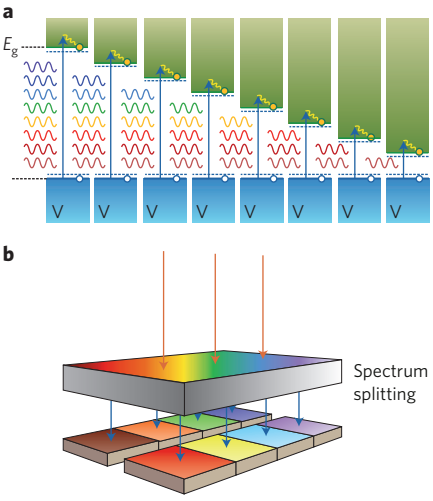

Figure 3 | Multi-junction solar cells. **a**, Multi-junction energy diagram. Semiconductors with different bandgaps convert different portions of the solar spectrum to reduce thermalization losses. The quasi-Fermi levels defining the open-circuit voltage are indicated by the horizontal blue dashed lines. The yellow dots represent the electrons. **b**, Parallel-connected architecture that can be realized using epitaxial liftoff and printing techniques of the semiconductor layers, followed by printing of a micro- or nanophotonic spectrum splitting layer. Each semiconductor layer can be combined with one of the structures in Fig. 2 to reduce entropy losses and these structures can be separately optimized for each semiconductor.

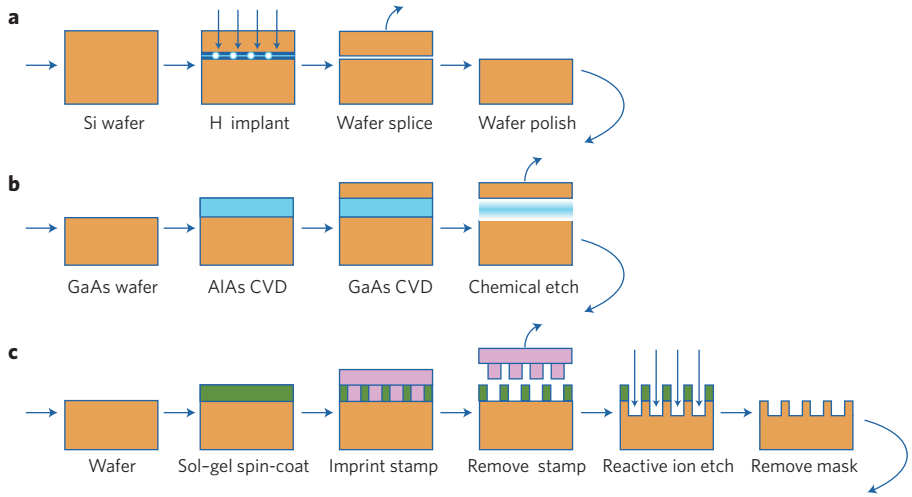

Figure 4 | Scalable inexpensive large-area layer transfer and nanofabrication techniques. **a**, Fabrication of ultrathin silicon wafers: hydrogen-ion implantation into a silicon wafer followed by annealing leads to formation of hydrogen bubbles at a well defined depth; the surface silicon layer can subsequently be peeled off and the remaining wafer is polished for re-use. **b**, Fabrication of ultrathin GaAs layers: AlAs (blue) and GaAs (orange) layers are epitaxially grown onto a GaAs substrate by chemical vapour deposition (CVD). Selective chemical etching removes the AlAs layer, subsequently the GaAs layer is lifted-off. In the lift-off processes in **a** and **b**, the thin layer is often laminated to a flexible substrate before it is peeled off. **c**, Soft-imprint lithography: a patterned rubber stamp (pink) is printed into a sol–gel layer (green) that is spin-coated onto the substrate. On drying of the sol–gel the stamp is removed and the pattern is transferred into the wafer by reactive-ion etching and the mask is removed. Using soft imprinting a spatial resolution of 10 nm is routinely achieved over a full 6″ wafer.

single-junction solar cell with appropriate light management.

To reach this goal, the solar-cell architecture must be radically modified. Several recent developments have laid the groundwork to reach this goal, in particular the explosion of scientific effort on light trapping and concentration using wavelength-scale and subwavelength optical elements, and, at the same time, the development of scalable large-area nanofabrication methods[16,17]. First, light directors must be integrated at the surface to redirect any radiative emission back within a solid angle corresponding to the disk of the Sun to minimize the first entropy term in equation (1). Microparabolic light reflectors that have been recently realized may serve this goal[18]. Alternatively, planar plasmonic or dielectric structures that serve as light collectors and antennas in the radiating mode[19,20] may also be suitable. Some of these possible designs are shown in Fig. 2a,b. Second, perfect light trapping must be achieved (second entropy term in equation (1)), which can be done by integrating a suitable surface texture with the cell. This is a standard technique for thick, wafer-based Si solar cells. Developments using nanopatterning (Fig. 2c)[21] also enable excellent light trapping in ultrathin semiconductor slabs in which the ray optics limit does not hold and light propagation is described by near-field effects and waveguide modes[22]. Third, the quantum efficiency (last entropy term in equation (1)) has reached near-unity values in, for example GaAs, thus not leaving much room for improvement. However, for Si, non-radiative recombination is significant and light management can be used to enhance the QE by enhancing the optical density of states, for example by engineering the modal dispersion in a thin-film solar cell or a plasmonic metal–insulator–metal geometry (Fig. 2d).

The second key factor limiting solar-cell performance is carrier thermalization: for a given semiconductor, light with a photon energy $E = \hbar\omega$ above the bandgap can only create a photovoltage V_{oc}, so that the mismatch energy $E - qV_{oc}$ is lost to heat (Fig. 1). Moreover, photons with an energy below the bandgap are not absorbed. This 'quantum defect' problem can be alleviated in a multi-junction geometry, in which different spectral bands from the solar spectrum are absorbed in different semiconductors with corresponding bandgaps (Fig. 3a). Conventionally, multi-junction solar cells are made in a series-connected architecture, with each subcell acting as a 'filter' collecting a spectral band corresponding to the electronic bandgap of each semiconductor layer. A disadvantage of this design is that complex and expensive ultrahigh-vacuum crystal-growth techniques are required to epitaxially grow the single-crystalline semiconductor layers as well as the intermediate tunnel barrier buffer layers. Moreover, in the series-connected architecture current-matching among the subcells is required, meaning that the subcell generating the lowest current limits the overall multi-junction cell current. Furthermore, the lattice-matched crystal-growth process limits the semiconductor materials composition. Also, the optically series-connected configuration dictates that each subcell is subject to the same light-concentration factor, an additional constraint reducing power-generation efficiency.

An alternative approach is shown in Fig. 3b; a design for a multi-junction photovoltaic architecture featuring an optically-in-parallel array of high-efficiency single-junction cells that form the receiver of a spectrum-splitting photonic structure[23]. This architecture has been explored preliminarily by the very high efficiency solar cell (VHESC) project[24], but many innovations are possible[25]. In this architecture the spectrum-splitting structure directs light of different wavelengths to individual subcells that are optimized for the corresponding spectral bands and concentration factor, with no limitations due to current matching, and with full flexibility in the choice of semiconductor material for the different subcells. Furthermore, although conventional multi-junction cells have employed three or four subcells, and the overall thermalization loss is still substantial, the alternative depicted in Fig. 3b can easily accommodate a larger number of subcells. If narrow (<300 meV) spectral bands from a spectrum-splitting photonic structure can be efficiently directed to an array with 8–10 types of subcell, thermalization can be limited to approximately 10%.

So far, macroscopic optical elements have been employed as light concentrators and spectral splitters in high-efficiency series-connected multi-junction photovoltaic systems. These optical elements thus operate using ray-optical principles for focusing and optical dispersion, for example using dichroic filters. Recently, photonic materials researchers have developed an extensive portfolio of design principles and methods to generate subwavelength optically dispersive and resonant light-trapping structures, including photonic crystal and plasmonic metamaterial designs, transformation optics and resonant-guided wave networks. We propose that these nano- and microphotonic design principles

can be used to develop spectral splitters and integrate them with the subcells to realize the planar, optically-in-parallel architecture in Fig. 3b. In a further advanced design, the subcells can be integrated with dedicated photonic structures that enable light trapping and angular restriction of emitted photons optimized for each subcell, thus also mitigating entropy losses in photon-to-electron conversion described above.

At first sight, the architecture in Fig. 3b seems relatively complex, as it involves the layer-transfer of multiple ultrathin semiconductor slabs, their integration with a microphotonic spectrum-splitting structure, and the realization of an electrical interconnection scheme. However, similarly complex architectures are routinely made today in components in optical telecommunication networks, where photonic integrated circuits such as wavelength-division multiplexers, optical splitters, filters and detector arrays are fabricated on a single chip. Indeed, in the new ultrahigh-efficiency solar-cell design proposed here, the solar cell must be seen as a complex optical integrated circuit that is optimized to convert light from the Sun to electricity.

The planar multi-junction design can be realized in a practical and scalable way using recent advances in the research and commercial development of epitaxial liftoff[26] and layer-transfer printing techniques for thin-film single-crystal Si and III–V compound semiconductor absorbers (Fig. 4a,b). Indeed, using epitaxial liftoff, world-record 1-sun single-junction solar-cell efficiencies have been recently achieved[1]; near-record efficiencies have been obtained using cells fabricated by transfer printing[27]. Furthermore, we note that soft-imprint lithography provides a scalable method for the synthesis of low-cost large-area arrays of nanopatterned light directors, light-trapping structures or structures with engineered optical density of states (Fig. 4c). It is now well established that soft-imprint lithography has a deep-subwavelength resolution, maintained over a large area, which is required to realize the light-management structures described here.

In conclusion, we describe several solar-cell architectural features that may pave the way towards achieving ultrahigh-efficiency photovoltaics. Our current work at the DOE Light–Material Interactions in Energy Conversion Center at CALTECH and the Light Management in new Photovoltaics Materials Programme at AMOLF is centred on investigation of these structures for improved solar-energy conversion. Whereas much effort in the past has focused on materials and device design in photovoltaics, we suggest that renewed focus on the science and technology of nano- and microphotonics for light management inside the solar cell has considerable potential. The photonic architectures described here address several distinct entropic and energy losses incurred in a conventional solar cell, as summarized in Fig. 5. Although many practical challenges await, the directions described here have considerable potential to enable very high photovoltaic efficiencies that have previously only been a wish rather than a concrete objective. ❐

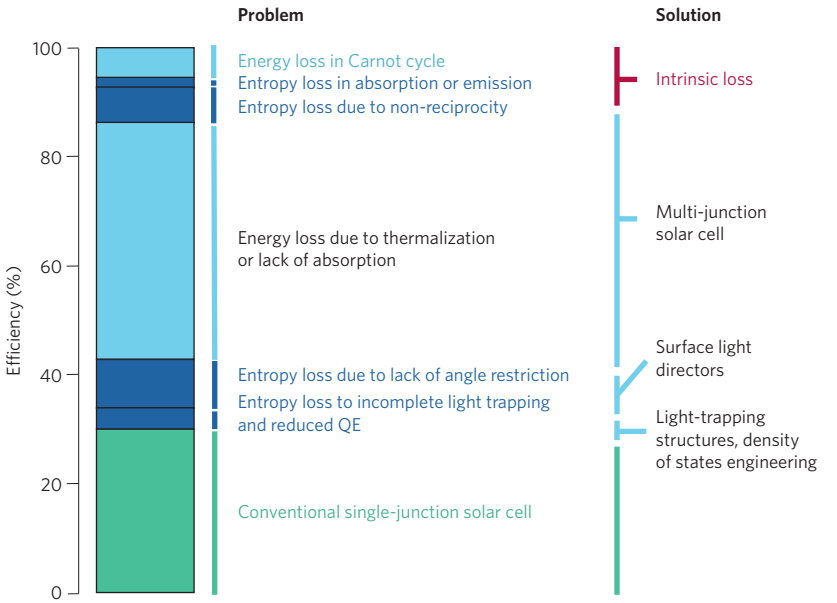

Figure 5 | Thermodynamic losses in solar-energy conversion. The maximum efficiency realized for a conventional single-junction solar cell is 28.3% (indicated in green). Dark blue bars indicate entropy-related losses and light blue bars indicate energy-related losses. The main energy loss is due to thermalization and lack of absorption. The solutions to reducing the entropy- and energy-loss problems are listed in the right-hand column.

Albert Polman is in the FOM Institute AMOLF, Science Park 104, 1098 XG Amsterdam, the Netherlands; Harry A. Atwater is in the California Institute of Technology, Pasadena California 91125, USA.
e-mail: polman@amolf.nl; haa@caltech.edu

References

1. Green, M. A., Emery, K., Hishikawa, Y., Warta, W. & Dunlop, E. D. *Prog. Photovolt. Res. Appl.* **20,** 12–20 (2012).
2. Yuen, H. in *Renewable Energy and the Environment* SRWB3 (OSA Technical Digest, 2011).
3. *Technology Roadmap — Solar Photovoltaic Energy* (International Energy Agency, 2010); http://www.iea.org/papers/2010/pv_roadmap.pdf
4. Shockley, W. & Queisser, H. J. *J. Appl. Phys.* **32,** 510–519 (1961).
5. Green, M. A. *Third-generation Photovoltaics: Advanced Solar Energy Conversion* (Springer, 2006).
6. Martí, A. & Luque, A. *Next Generation Photovoltaics: High Efficiency through Full Spectrum Utilization* (Institute of Physics, 2003).
7. Landsberg, P. T. & Tonge, G. *J. Appl. Phys.* **51,** R1–R20 (1980).
8. Ruppel, W. & Würfel, P. *IEEE Trans. Electron. Dev.* **27,** 877–882 (1980).
9. Würfel, P. *Physica E* **14,** 18–26 (2002).
10. Campbell, P. & Green, M. A. *IEEE Trans. Elec. Dev.* **33,** 234–239 (1986).
11. Araújo, G. L. & Martí, A. *Solar Energy Mater. Solar Cells* **33,** 213–240 (1994).
12. Tiedje, T., Yablonovitch, E., Cody, G. D. & Brooks, B. G. *IEEE Trans. Electron. Dev.* **31,** 711–716 (1984).
13. Yablonovitch, E. *J. Opt. Soc. Am.* **72,** 899–907 (1982).
14. Yu, Z. F., Raman, A. & Fan, S. H. *Proc. Natl Acad. Sci. USA* **107,** 17491–17496 (2010).
15. Callahan, D. M., Munday, J. N. & Atwater, H. A. *Nano Lett.* **12,** 214 (2011).
16. Luque, A. *Solar Energy Mater. Solar Cells* **23,** 152–163 (1991).
17. Atwater, H. A. & Polman, A. *Nature Mater.* **9,** 205–213 (2010).
18. Atwater, J. H. *et al. Appl. Phys. Lett.* **99,** 151113 (2011).
19. Laux, E., Genet, C., Skauli, T. & Ebbesen, T. W. *Nature Photon.* **2,** 161–164 (2008).
20. Coenen, T., Vesseur, E. J. R. & Polman, A. *ACS Nano* http://dx.doi.org/10.1021/nn204750d (2012).
21. Spinelli, P., Verschuuren, M. A. & Polman, A. *Nature Commun.* http://dx.doi.org/ 10.1038/ncomms1691 (in the press).
22. Ferry, V. E. *et al. Nano Lett.* **11,** 4239–4245 (2011).
23. Imenes, A. G. & Mills, D. R. *Solar Energy Mater. Solar Cells* **84,** 19–69 (2004).
24. Barnett, A. *et al. Prog. Photovolt. Res. Appl.* **17,** 75–83 (2009).
25. Green, M. A. & Ho-Baille, A. *Prog. Photovolt. Res. Appl.* **18,** 42–47 (2010).
26. Yablonovitch, E., Hwang, D. M., Gmitter, T. J., Florez, L. T. & Harbison, J. P. *Appl. Phys. Lett.* **56,** 2419–2421 (1990).
27. Yoon, J. *et al. Nature* **465,** 329–333 (2010).

Acknowledgements

The authors acknowledge helpful discussions with Eli Yablonovitch, John Rogers, Paul Braun, Nathan S. Lewis, Ralph Nuzzo and Enrique Canovas. The Caltech portion of this work was supported by DOE Office of Basic Energy Sciences 'Light–Material Interactions in Energy Conversion' Energy Frontier Research Center under grant DE-SC0001293. Work at AMOLF is part of the research programme of FOM which is financially supported by NWO; it is also supported by the European Research Council. This work is also part of the Global Climate and Energy Project (GCEP).